Applied Thermal Engineering ■■ (2016) ■■–■■

Contents lists available at ScienceDirect

Applied Thermal Engineering

journal homepage: www.elsevier.com/locate/apthermeng

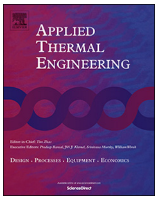

Multi-objective operation optimization of a Distributed Energy System for a large-scale utility customer

Marialaura Di Somma [a,b,*], Bing Yan [c], Nicola Bianco [a], Peter B. Luh [c], Giorgio Graditi [b], Luigi Mongibello [b], Vincenzo Naso [a]

[a] *Dipartimento di Ingegneria Industriale (DII), Università degli Studi Federico II, Napoli 80125, Italy*
[b] *ENEA, Italian National Agency for New Technologies, Energy and Sustainable Economic Development, CR Portici, Portici 80055, Italy*
[c] *Department of Electrical and Computer Engineering, University of Connecticut, Storrs, CT 06269, USA*

HIGHLIGHTS

- Multi-objective operation optimization model of a Distributed Energy System.
- Optimized operation strategies to reduce energy costs and environmental impacts.
- Method implemented for a large-scale utility customer as end-user.
- Energy costs and CO_2 emissions reduced by the optimized operation.

ARTICLE INFO

Article history:
Received 2 September 2015
Accepted 7 February 2016
Available online

Keywords:
Distributed Energy System
Total energy cost and CO_2 emission
Multi-objective operation optimization

ABSTRACT

With energy saving issues and growing environment protection awareness, interests in distributed generation have been intensifying. Distributed Energy Systems (DESs) are being widely investigated, since they are expected to be largely used to increase the efficiency of energy supply and to address environmental problems. In this paper, a multi-objective optimization problem is formulated to obtain the optimized operation strategies of a DES, to reduce both energy costs and environmental impacts. The DES includes different energy conversion devices and thermal energy storage systems to satisfy time-varying user demands. The Pareto front, including the best possible trade-offs between the economic and the environmental objectives, is obtained by minimizing a weighted sum of the total energy costs and CO_2 emissions. The operators of DESs can choose the operation strategy from the Pareto front based on the economic and environmental priorities. The method is implemented for a DES with a large-scale utility customer as end-user. Results show that the optimized operation of the DES reduces energy costs and CO_2 emissions, as compared with conventional energy supply systems. In addition, a sensitivity analysis is carried out to analyze the effects on energy costs and environmental impacts of variations in the configuration of the DES.

1. Introduction

A Distributed Energy System (DES) may consist of small-scale heat and power generation technologies including also renewable ones, and storage units, providing electric and thermal energy to end-users [1]. In recent years, interest has been intensifying in the development of DESs, which are considered as an efficient and environmental friendly alternative to conventional energy supply systems [1–6]. These systems, with appropriate design and operation strategies, may exhibit even better performances than a single polygeneration energy system (e.g., combined heat and power) or conventional energy supply systems. For instance, integration with renewable energy resources may lead to environmental benefits and efficient use of energy resources. However, most of the studies in the literature have been focused on the optimization of specific energy systems as combined heat and power systems and their operation strategies [7–11]. Most of literature on DESs has been focused on their operation optimization from the economic point of view. Among them, integrated optimization of energy devices and energy processes of a small eco-community was carried out in Yan et al. [12] to reduce the total energy costs. The solution methodology used was branch-and-cut. A mixed-integer optimization model for scheduling multiple energy devices connected to a low energy building was developed in Guan et al. [13] to minimize the overall costs of

---

[*] Corresponding author. Tel.: +39 0817723204, +39 3492963733; fax: +39 0817723344.
E-mail addresses: marialaura.disomma@unina.it, marialaura.disomma@enea.it (M. Di Somma).

http://dx.doi.org/10.1016/j.applthermaleng.2016.02.027
1359-4311/

Please cite this article in press as: Marialaura Di Somma, et al., Multi-objective operation optimization of a Distributed Energy System for a large-scale utility customer, Applied Thermal Engineering (2016), doi: 10.1016/j.applthermaleng.2016.02.027

electricity and natural gas. The problem was also solved by branch-and-cut.

The economic analysis alone is not sufficient due to growing environmental concerns, like the global warming and the depletion of fossil fuels. Operation problems of DESs, including different energy systems, become more challenging when the environmental aspects are also taken into account, since the economic and the environmental objectives may be contradictory [14,15]. In addition, the energy devices involved convert and store different energy carriers (e.g., electricity, natural gas, solar energy, hot and/or cold fluids) with different energy efficiencies and environmental impacts.

In this paper, a multi-objective linear programming (MOLP) problem is formulated to obtain the optimized operation strategies of a DES to reduce the energy costs and environmental impacts, while satisfying time-varying user demands, with given prices of energy sources. The DES involves different energy conversion devices: Combined Cooling Heat and Power (CCHP) system, solar thermal plant, reversible heat pump and thermal energy storage systems, which provide electricity, heat and cooling to end-users. The economic objective is formulated as the total energy cost to be minimized, and the environmental objective is formulated as the total CO_2 emission to be minimized. The Pareto front involving the best possible trade-offs between the economic and environmental objectives is obtained by minimizing a weighted sum of the total energy cost and CO_2 emission, by using branch-and-cut. The operators of DESs can choose the operation strategy from the Pareto front based on the economic and environmental priorities.

As an illustrative example, a large-scale utility customer (a large hotel located in Italy) is considered as the end-user. Results show that the optimized operation of the DES allows to reduce energy costs and environmental impacts, as compared with conventional energy supply systems. In addition, a sensitivity analysis is carried out to analyze the effects on energy costs and environmental impacts of variations in the configuration of the DES.

2. Problem formulation

The DES under consideration consists of energy conversion devices and thermal energy storage systems, providing electricity, heat and cooling to end-users. Fig. 1 shows the scheme of the DES with the possible routes of energy carriers from various energy resources via primary and secondary energy devices, and thermal energy storage systems to meet given time-varying user demands. Modeling of energy devices and thermal storage is presented in subsection 2.1, and energy balances are described in subsection 2.2.

2.1. Modeling of energy devices and thermal storage

The common constraint for most of the energy devices is the capacity constraint, formulated as follows:

$$x_{ED}(t)k_{ED}^{\min} \le k_{ED}(t) \le x_{ED}(t)k_{ED}^{\max}, \tag{1}$$

which means that if the energy device is in use (i.e., the on/off binary decision variable, $x_{ED}(t)$, is 1), its generation level (the decision variable), $k_{ED}(t)$, has to be within the minimum value, $k_{ED}^{\min}$, and its capacity, $k_{ED}^{\max}$, and 0 when the energy device is off.

Additional constraints for CCHP, solar thermal plant, reversible heat pump and thermal storage are presented in the following.

2.1.1. Modeling of the CCHP system

The CCHP system consists of an Internal Combustion Engine (ICE); two heat recovery boilers, for Domestic Hot Water (DHW) and Space Heating (SH) demands, respectively; an absorption chiller, for Space Cooling (SC) demand, as sketched inside the bold lines in Fig. 1. The internal combustion engine provides electricity fueled by natural gas. Thermal energy is recovered from exhaust gas and used to provide heating by the heat recovery boilers and cooling by the absorption chiller. Furthermore, heating and cooling can be also directly generated by supplementary burning of natural gas in the boilers and absorption chiller, respectively [16]. Decision variables for the CCHP system are the electricity generation level in the internal combustion engine, the fraction of exhaust gas for domestic hot water, space heating and cooling demands, and heating and cooling directly provided by supplementary burning of natural gas in the boilers and absorption chiller, respectively.

Constraints considered for the CCHP system are presented below. The volumetric flow rate of natural gas, $\dot{G}_{ICE}(t)$, required by the engine to provide electricity, $\dot{E}_{CCHP}(t)$, is given by:

$$\dot{G}_{ICE}(t) = \dot{E}_{CCHP}(t) / (\eta_e LHV_{gas}), \tag{2}$$

where η_e is the engine gas-to-electric efficiency and LHV_{gas} is the lower heat value of natural gas. In Eq. (2), $\dot{G}_{ICE}(t)$ is expressed in Nm^3/h, where Nm^3 stands for the volume of gas at 0 °C temperature and at 1.013 bar pressure.

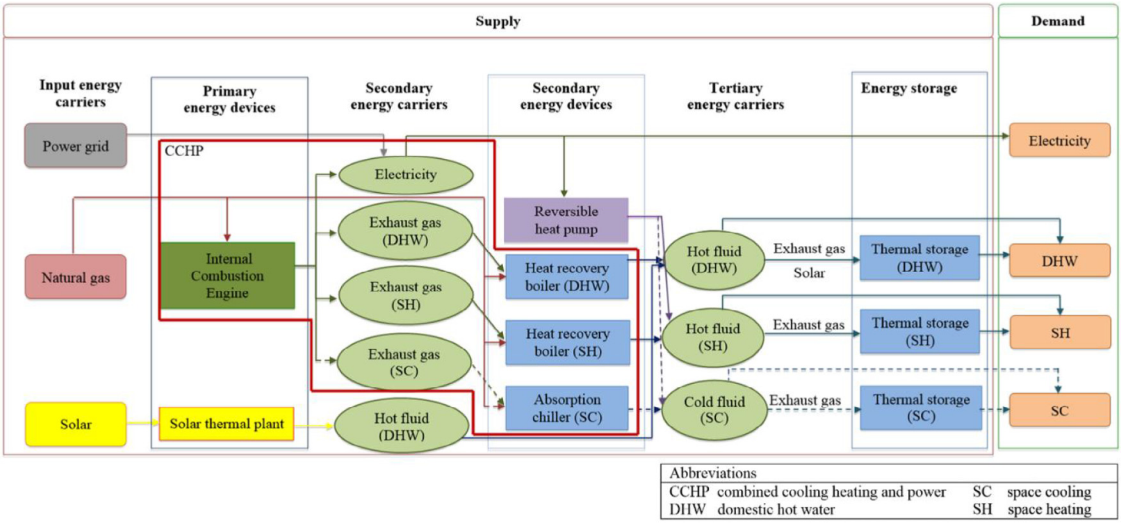

Fig. 1. Scheme of the DES for the optimization problem.

Please cite this article in press as: Marialaura Di Somma, et al., Multi-objective operation optimization of a Distributed Energy System for a large-scale utility customer, Applied Thermal Engineering (2016), doi: 10.1016/j.applthermaleng.2016.02.027

The heat rate available from the exhaust gas recovered from the engine, $\dot{Q}_{ICE,ex}(t)$, is:

$$\dot{Q}_{ICE,ex}(t) = \dot{E}_{CCHP}(t)(1 - \eta_e - \mu_{ICE})/\eta_e, \tag{3}$$

where μ_{ICE} is the percent heat loss of the engine.

Engine exhaust gas can be subdivided among the heat recovery boilers and the absorption chiller to supply heating for the domestic hot water and space heating demands as well as cooling for the space cooling demand.

The heat rate supplied by the exhaust gas to the heat recovery boiler for the domestic hot water demand, $\dot{H}_{ex}^{DHW}(t)$, is:

$$\dot{H}_{ex}^{DHW}(t) = \dot{Q}_{ICE,ex}(t)\xi_{DHW}(t)\eta_{HR,boil}, \tag{4}$$

where $\eta_{HR,boil}$ is the efficiency of the heat recovery boiler, and the continuous decision variable, $\xi_{DHW}(t)$, is the fraction of exhaust gas supplied to the heat recovery boiler for the domestic hot water demand.

Heating can be also directly provided by supplementary burning of natural gas in the heat recovery boiler. The volumetric flow rate of natural gas, $\dot{G}_{boil}^{DHW}(t)$, required by the boiler to directly provide the heat rate, $\dot{H}_{di}^{DHW}(t)$, is:

$$\dot{G}_{boil}^{DHW}(t) = \dot{H}_{di}^{DHW}(t)/(\eta_{boil} LHV_{gas}), \tag{5}$$

where η_{boil} is the combustion efficiency of the boiler.

Therefore, the total generation of the heat recovery boiler for the domestic hot water demand, $\dot{H}_{CCHP}^{DHW}(t)$, is the sum of the heat rate obtained by exhaust gas, $\dot{H}_{ex}^{DHW}(t)$, and the heat rate directly provided by supplementary burning of natural gas, $\dot{H}_{di}^{DHW}(t)$:

$$\dot{H}_{CCHP}^{DHW}(t) = \dot{H}_{ex}^{DHW}(t) + \dot{H}_{di}^{DHW}(t). \tag{6}$$

Modeling of heating for the space heating demand and of cooling for the space cooling demand by the CCHP system is similar to that described above.

The sum of the engine exhaust gas fractions used for domestic hot water, $\xi_{DHW}(t)$, space heating, $\xi_{SH}(t)$, in the heat recovery boilers, and space cooling, $\xi_{SC}(t)$, in the absorption chiller, has to be one:

$$\xi_{DHW}(t) + \xi_{SH}(t) + \xi_{SC}(t) = 1. \tag{7}$$

The overall volumetric flow rate of natural gas consumed by the CCHP system, $\dot{G}_{CCHP}(t)$, is:

$$\dot{G}_{CCHP}(t) = \dot{G}_{ICE}(t) + \dot{G}_{boil}^{DHW}(t) + \dot{G}_{boil}^{SH}(t) + \dot{G}_{abs}(t), \tag{8}$$

where $\dot{G}_{boil}^{SH}(t)$ is the volumetric flow rate of natural gas required by the boiler to directly provide heating for the space heating demand, and $\dot{G}_{abs}(t)$ is the volumetric flow rate of natural gas required by the absorption chiller to directly provide cooling for the space cooling demand.

2.1.2. *Modeling of the solar thermal plant*

A solar thermal plant is used to meet the domestic hot water demand. The heat rate provided by the solar plant, $\dot{H}_{solar}(t)$, depends on the collector area, A_{coll}, its efficiency, η_{coll}, and the total solar irradiance, $\dot{G}_T(t)$, and is expressed by:

$$\dot{H}_{solar}(t) = \eta_{coll} A_{coll} \dot{G}_T(t), \tag{9}$$

where the collector area is assumed known, since the optimal design of the DES is not the aim of this work.

2.1.3. *Modeling of the reversible heat pump*

A reversible heat pump is used to meet space heating and cooling demands in the heating and cooling modes, respectively. In the heating mode, the electricity consumption of the heat pump, $\dot{E}_{HP}(t)$, to supply the heat rate, $\dot{H}_{HP}(t)$, is given by:

$$\dot{E}_{HP}(t) = \dot{H}_{HP}(t)/COP_{HP}, \tag{10}$$

where COP_{HP} is the coefficient of performance of the heat pump in the heating mode. Modeling of the cooling mode is similar to that described above.

2.1.4. *Modeling of thermal energy storage systems*

The energy stored in the domestic hot water tank at time t, $H_{sto}(t)$, can be expressed as:

$$H_{sto}(t) = H_{sto}(t - \Delta t)\eta_{sto} + \left(\dot{H}_{sto}^{in}(t) - \dot{H}_{sto}^{out}(t)\right)\Delta t, \tag{11}$$

where η_{sto} is the efficiency of the thermal storage and Δt is the length of the time interval. The decision variables are $\dot{H}_{sto}^{in}(t)$ and $\dot{H}_{sto}^{out}(t)$, which are the heat rates brought in and taken out by the flow-in and flow-out water, respectively.

It is assumed that there are three different thermal energy storage systems, each of them for the corresponding thermal energy demand. Modeling of thermal storage systems for space heating and cooling is similar to the above.

2.2. *Modeling of energy balances*

In order to satisfy the given time-varying user demands, electricity and thermal energy balances are formulated by matching supply and demand.

2.2.1. *Electricity balance*

The electricity rate demand, $\dot{E}_{dem}(t)$, and the electricity rate required by the heat pump, $\dot{E}_{HP}(t)$, must be covered by the sum of the electricity rate delivered by the CCHP system, $\dot{E}_{CCHP}(t)$, and the electricity rate bought from the grid (a continuous decision variable), $\dot{E}_{buy}(t)$:

$$\dot{E}_{dem}(t) + \dot{E}_{HP}(t) = \dot{E}_{CCHP}(t) + \dot{E}_{buy}(t). \tag{12}$$

2.2.2. *Domestic hot water energy balance*

The heat rate demanded for domestic hot water, $\dot{H}_{dem}^{DHW}(t)$, must be satisfied by the total heat rate provided by the CCHP system, $\dot{H}_{CCHP}^{DHW}(t)$, by the solar thermal plant, $\dot{H}_{solar}(t)$, and by the thermal storage, $\dot{H}_{sto}^{out}(t) - \dot{H}_{sto}^{in}(t)$, that is:

$$\dot{H}_{dem}^{DHW}(t) = \dot{H}_{CCHP}^{DHW}(t) + \dot{H}_{solar}(t) + \dot{H}_{sto}^{out}(t) - \dot{H}_{sto}^{in}(t). \tag{13}$$

The space heating and cooling balances can be expressed in a similar way.

3. Multi-objective optimization

The objective is to minimize the total energy costs and CO_2 emissions. The economic and environmental objective functions are discussed in subsection 3.1. To solve the problem, the multi-objective optimization method is discussed in subsection 3.2.

3.1. *Economic and environmental objectives*

The economic objective is to minimize the total energy cost, *Cost*, that is the cost of the gas consumed by the CCHP system, $\dot{G}_{CCHP}(t)$, and the cost of the grid power, $E_{buy}(t)$:

Please cite this article in press as: Marialaura Di Somma, et al., Multi-objective operation optimization of a Distributed Energy System for a large-scale utility customer, Applied Thermal Engineering (2016), doi: 10.1016/j.applthermaleng.2016.02.027

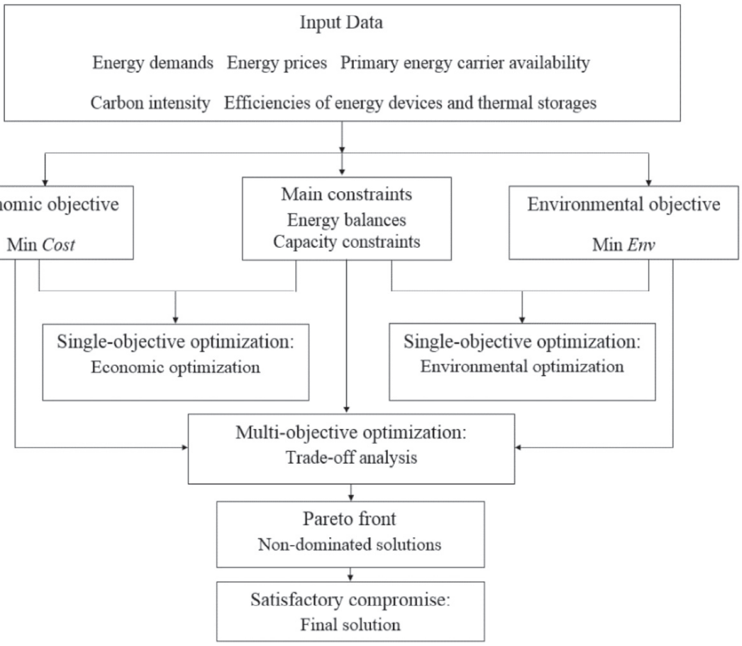

Fig. 2. Flowchart of the multi-objective optimization model.

$$Cost = \sum_t \left(P_{grid}(t)\dot{E}_{buy}(t) + P_{gas}\dot{G}_{CCHP}(t)\right)\Delta t, \tag{14}$$

where $P_{grid}(t)$ is the time-of-day unit price of electricity from the grid and P_{gas} is the constant unit price of natural gas.

The environmental objective is to minimize the environmental impacts, *Env*, in terms of CO_2 emission from the power grid and the consumed fuels. The CO_2 emission due to the use of electricity from the power grid is evaluated by multiplying the carbon intensity of the power grid, E_{cin}, and the total amount of electricity from the grid, $\dot{E}_{buy}(t)$. The carbon intensity of the power grid that the DES is connected to is the amount of CO_2 emission per unit of electricity generated which depends on the fuel mix. The CO_2 emission due to the natural gas consumption is evaluated by multiplying the carbon intensity of the fuel, G_{cin}, and the total amount of fuel consumption of the CCHP system, $\dot{G}_{CCHP}(t)$ [17]. Therefore, the total CO_2 emission is expressed as follows,

$$Env = \sum_t \left(E_{cin}\dot{E}_{buy}(t) + G_{cin}\dot{G}_{CCHP}(t)\right)\Delta t. \tag{15}$$

3.2. Multi-objective optimization method

With the economic objective function (Eq. 14) and the environmental one (Eq. 15), the problem has two objective functions to be minimized. To solve this multi-objective problem, a single objective function is formulated as a weighted sum of the total energy cost, *Cost*, and the environmental impacts, *Env*, to be minimized:

$$F_{obj} = c\omega Cost + (1-\omega)Env, \tag{16}$$

where the constant c is chosen such that c *Cost* and *Env* have the same order of magnitude. For $\omega = 1$, the economic optimization is carried out and the solution that minimizes the total energy cost can be found. For $\omega = 0$, the environmental impact optimization is carried out and the solution that minimizes the total CO_2 emission can be found. Then, the constant c is calculated as the ratio of the maximum total CO_2 emission obtained by the economic optimization to the maximum total energy cost obtained by the environmental impact optimization. With the constant c, the Pareto front involving the best possible trade-offs between the two objectives can be found by varying the weight ω in between the interval 0 and 1. The problem formulated above is linear and involves both discrete and continuous variables. This mixed integer linear programming problem is solved by branch-and-cut. Fig. 2 shows the flowchart to find the optimized operation strategies of the DES, with both economic and environmental objectives. Given the input data, by solving the above problem, the Pareto front, consisting of the best possible trade-offs between the two objectives, can be obtained. Each point of the Pareto front corresponds to a different operation strategy of the DES. The operators of DESs can choose the operation strategy from the Pareto front based on the economic and environmental priorities.

4. Numerical testing

The above formulated problem has been implemented by using IBM ILOG CPLEX Optimization Studio Version 12.5. As an illustrative example, a hypothetical large hotel of 16,000 m^2 located in Italy (D climatic zone [18]) is considered as the targeted end-user. In Europe, hotel facilities are ranked among the top five in terms of energy consumption in the tertiary building sector [19]. Moreover, in Italy, interest has been intensifying in promoting DESs, as demonstrated by several research and demonstration projects [20–23]. A typical winter day is chosen, with one hour as timestep. The configuration of the DES, including the sizes of energy devices, is sketched in Fig. 3.

4.1. Model inputs

The required inputs for the optimization model are demands information, energy prices, primary energy carrier availability, carbon intensities, and efficiencies of energy devices and thermal storage, as discussed in the following.

Please cite this article in press as: Marialaura Di Somma, et al., Multi-objective operation optimization of a Distributed Energy System for a large-scale utility customer, Applied Thermal Engineering (2016), doi: 10.1016/j.applthermaleng.2016.02.027

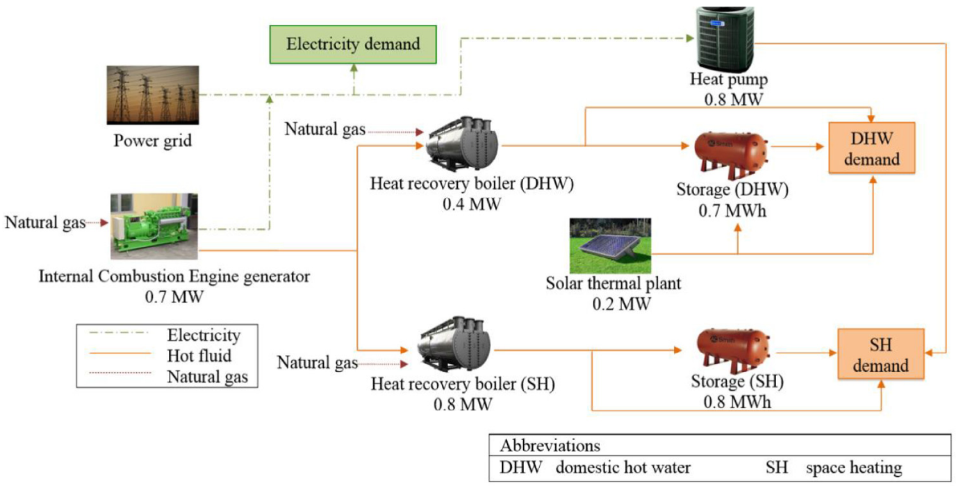

Fig. 3. DES configuration.

4.1.1. Energy demand

The hourly electricity, domestic hot water and space heating demands are taken from the literature [24–26]. The energy rate demand profiles for a typical winter day are reported in Fig. 4.

4.1.2. Energy prices

The time-of-day unit price of electricity from the power grid and the unit price of natural gas are chosen according to the current Italian market scenario. With reference to the Italian BTA6 tariff [27] for industrial use of electricity from the power grid, the unit price (€/kWh) accounts for the sum of the energy and dispatching prices, the power distribution and transmission quotas, the equalization component and the excise fee. The time-of-day grid price considered in this study is shown in Fig. 5. For the natural gas, the tariff for industrial use is adopted [28].

Reference is made to a unit price (€/Nm^3) consisting of the energy quotas (energy unit price and additional charges), the other variable quotas as distribution and transport sale quotas, and the excise fee.

4.1.3. Primary energy carriers

The energy carriers' input to the DES are electricity from the power grid, natural gas and solar energy. The first two are assumed unlimited, whereas the heat rate provided by the solar thermal plant is derived by the solar energy input taken from meteorological data for the considered location [29]. The hourly solar irradiance of a representative winter day is evaluated as the average of the solar irradiance in the corresponding hours of all winter days.

4.1.4. Carbon intensity

The carbon intensities of electricity from the power grid and natural gas are needed to evaluate the total amount of CO_2 emission related to the operation of the DES. The carbon intensity of the power grid is taken from Reference 30 equal to 0.354 kg/kWh, as the averaged value in the years 2009–2011 for Europe. The carbon intensity of natural gas is taken from Reference 17 equal to 0.202 kg/kWh.

4.1.5. Efficiency of energy devices and thermal storage

Typical efficiency values assumed for the energy devices and thermal storage are reported in Table 1. The temperature of exhaust gas from the internal combustion engine is assumed equal to 623.15 K and the temperature of exhaust gas at the exit of the heat recovery boiler is assumed equal to 363.15 K [17]. The efficiency of the heat recovery boiler is evaluated as the ratio of difference between the inlet and the outlet temperature of the engine exhaust

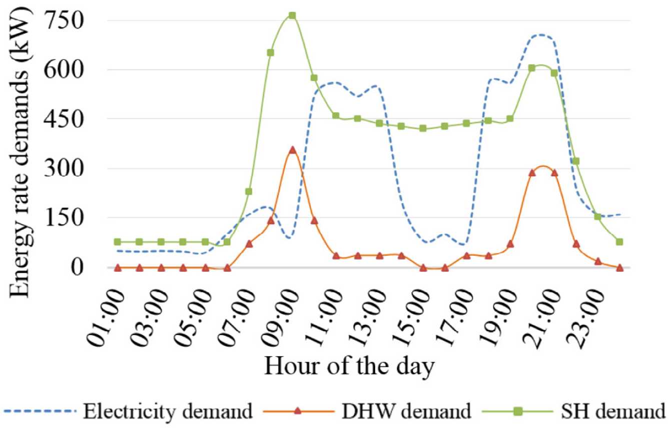

Fig. 4. Energy rate demands of a hypothetical hotel in Italy for a representative winter day.

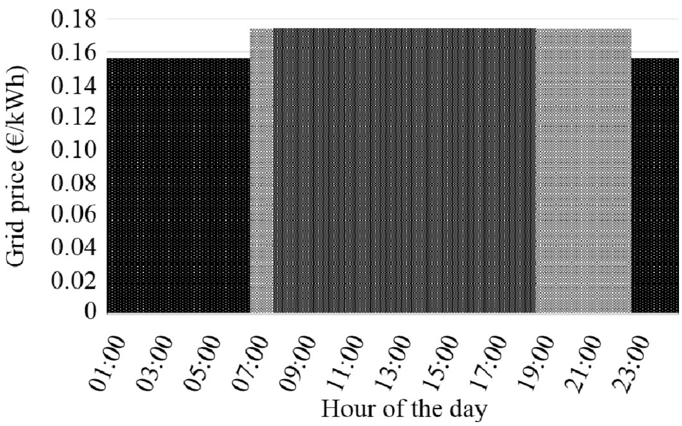

Fig. 5. Time-of-day grid price for industrial use [27].

Please cite this article in press as: Marialaura Di Somma, et al., Multi-objective operation optimization of a Distributed Energy System for a large-scale utility customer, Applied Thermal Engineering (2016), doi: 10.1016/j.applthermaleng.2016.02.027

Table 1
Efficiency of energy devices and thermal storage.

Primary energy devices	Efficiency	
	Electrical	Thermal
Internal combustion engine	0.35	0.50
Solar thermal plant		0.40
Secondary energy devices	Efficiency	
Heat pump	$COP_{HP} = 3.0$	
Heat recovery boiler	$\eta_{HRboil} = 0.75$, $\eta_{boil} = 0.85$	
Thermal energy storage		Efficiency
DHW and SH storage		0.90

gas in the heat recovery boiler to the difference between the inlet exhaust gas temperature and the ambient temperature.

4.2. Results

With the input data described above, the optimization method is implemented by using IBM ILOG CPLEX. The Pareto front involving the best possible trade-offs between the economic and the environmental objectives is presented in subsection 4.2.1. The optimized operation strategies of the DES under different weights for the two objectives are discussed in subsection 4.2.2.

4.2.1. Pareto front

Fig. 6 shows the Pareto fronts obtained without and with the discount on the excise fee of natural gas applicable to high-efficiency cogeneration systems (Primary Energy Saving (PES) > 0) [31]. In the first case, the natural gas tariff for industrial use described in subsection 4.1.2 is adopted, considering the excise fee for industrial use for all the natural gas consumed by the CCHP system [32]. In the second case, the discount on the excise fee for natural gas is involved, since the CCHP system has a PES > 0. According to Reference 32, this discount is applied to a 0.25 Nm^3 volumetric flow rate of natural gas consumed by the CCHP system for each kWh of electricity provided. The additional consumption of natural gas, which occurs when the CCHP system has an electrical efficiency less than 42%, is subjected to the industrial excise fee. Also, the natural gas consumed by the boilers to directly provide heating for the domestic hot water and space heating demands is subjected to the industrial excise fee [32].

In the first case (without discount on the excise fee of natural gas), the point marked with *a* is obtained by minimizing the daily energy cost, and the daily energy cost is 1260 €/d, whereas the daily CO$_2$ emission is 4160 kg/d. The point marked with *b* is obtained by minimizing the environmental impacts (the daily CO$_2$ emission), and the daily energy cost is 1594 €/d, whereas the daily CO$_2$ emission is 3448 kg/d. The points between the extreme points are found by equally subdividing the weight interval into 100 spaces.

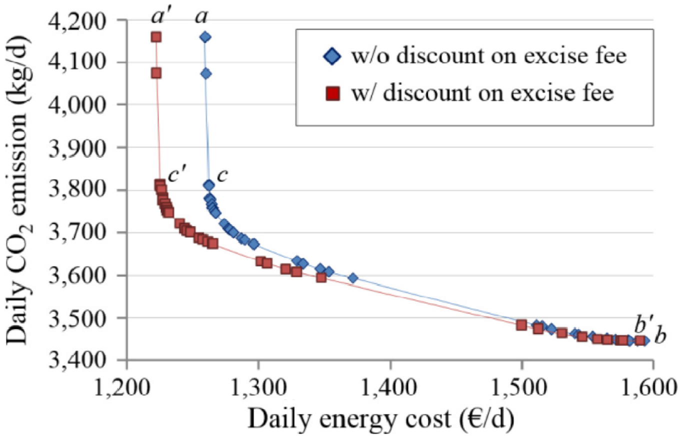

Fig. 6. Pareto fronts with and without discount on the excise fee of natural gas.

In the second case (with discount on the excise fee of natural gas), the Pareto front is obtained in the same way, where the points marked with *a′* and *b′* are obtained by minimizing the daily energy cost and the daily CO$_2$ emission, respectively. In both cases, a significant reduction, 8%, in the CO$_2$ emission is gained from solution points *a* and *a′* ($\omega = 1$) to the solution points *c* and *c′* ($\omega = 0.9$) with a negligible 0.25% increase in the energy cost. The differences between the two Pareto fronts become more significant when the weight for the economic objective increases (left side). In the energy cost minimization, at the point *a′*, the daily energy cost is 1223 €/d and it is reduced by about 3% as compared with the energy cost at the point *a*. The total CO$_2$ emission is the same as those at the point *a*. When the weight for the environmental objective increases, the sensitivity of the DES operation to the energy prices reduces, therefore the difference between the Pareto fronts reduces (right side). At the point *b′*, the daily energy cost is 1589 €/d and the daily CO$_2$ emission is the same as those at the point *b*, since, when the environmental objective is minimized, the operation of the DES is not sensitive to the energy prices. In the environmental impact minimization, the daily energy cost at the point *b′* is almost equal to that at the point *b*, because of the very small difference between the discounted excise and the full excise prices for industrial use.

4.2.2. Optimized operation strategies at various trade-off points

Each point on the Pareto front corresponds to a different operation strategy of the DES. The operators of the DES can choose a compromise between the two objectives from the Pareto front based on their cost and environmental priorities. In order to understand how the operation strategies of the DES affect the energy cost and the CO$_2$ emission under different weight values, the results at various trade-off points are shown in Fig. 7. These trade-off points belong to the Pareto front obtained when the discount on the excise fee is involved (red Pareto front in Fig. 6). Fig. 7a points out that, as ω increases from 0 to 1, the share of the electricity load (the sum of electricity demand and electricity rate required by the heat pump) satisfied by the CCHP significantly increases (5% to 59%), highlighting that the CCHP system allows to reduce the total energy cost. The opposite occurs to the share of electricity load covered by the grid power. The maximum value is obtained when the environmental impact is minimized, since the space heating demand is fully satisfied by the heat pump, as shown in Fig. 7c. As ω increases from 0 to 1, the share of the space heating demand satisfied by the heat pump decreases, whereas the share covered by the heat recovery boiler driven by exhaust gas increases because of the increase in the use of the CCHP system. In the energy cost minimization, the operation of the DES is only sensitive to energy prices, and the CCHP system instead of the power grid is mostly used to provide electricity.

It is also worth noting that Fig. 7a, 7b and 7c are strongly related. For instance, the CCHP system is rarely used in the environmental impact minimization, since the space heating demand is fully satisfied by the heat pump. Correspondingly, the heat rates from exhaust gas and the solar thermal plant do not satisfy the domestic hot water demand, and the integration with the boiler driven by natural gas is needed. As the use of the CCHP system increases and the use of the heat pump reduces, the amount of exhaust gas increases, and the integration with the boiler driven by natural gas is not needed. When the weight of the economic objective is close to 1 ($\omega = 0.8$ and $\omega = 0.9$), the natural gas boiler is used to satisfy a small share (3–5%) of the domestic hot water demand. Although in the economic optimization the use of the CCHP system reaches the maximum value, exhaust gas is not enough to satisfy the domes-

Please cite this article in press as: Marialaura Di Somma, et al., Multi-objective operation optimization of a Distributed Energy System for a large-scale utility customer, Applied Thermal Engineering (2016), doi: 10.1016/j.applthermaleng.2016.02.027

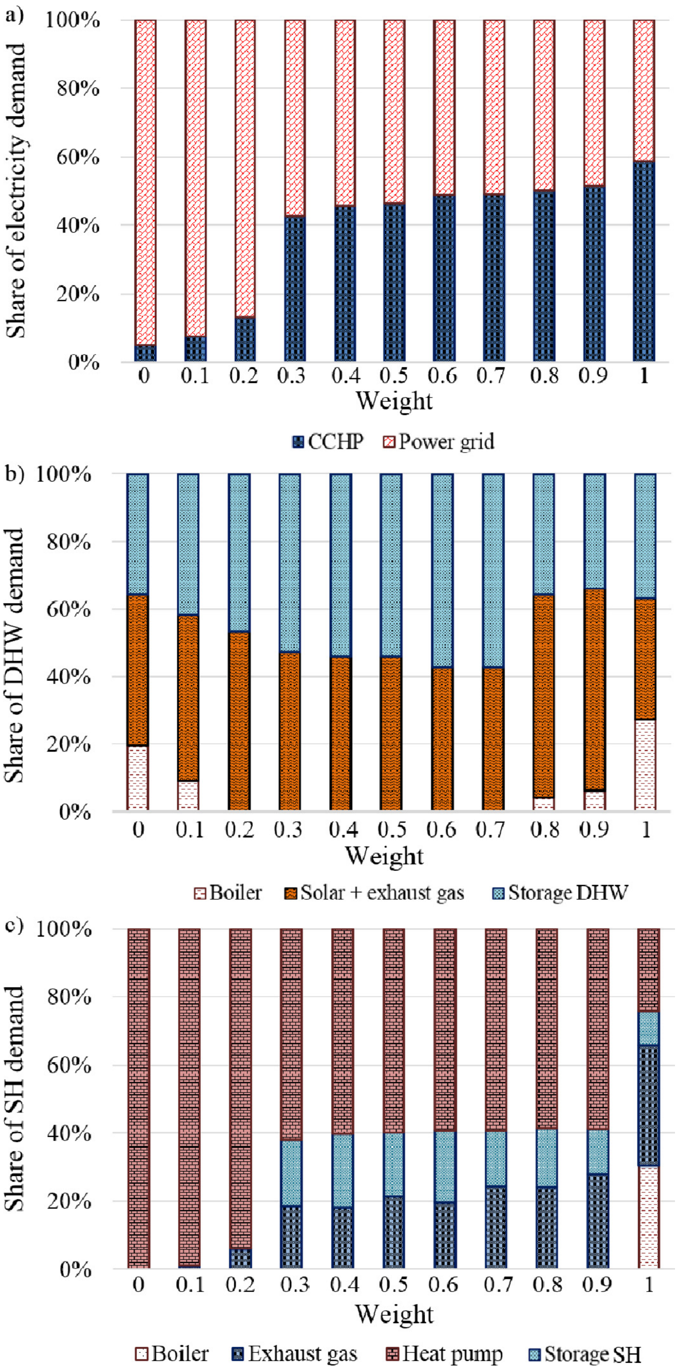

Fig. 7. Optimized operation strategies of the DES at various trade-off points for a) electricity, b) domestic hot water, c) space heating.

tic hot water and space heating demands. Therefore, the use of natural gas boilers significantly increases consistently with the reduction in the use of the heat pump. The remarkable difference in the operation of the DES from $\omega = 1$ to $\omega = 0.9$ corresponds to the big jump from a' to c' shown in Fig. 6.

4.3. Sensitivity analysis

A sensitivity analysis is carried out to analyze the effects on energy costs and environmental impacts of variations in the configuration of the DES.

Table 2
Investigated configurations.

Configuration	Energy devices excluded from the reference case (Configuration 1)
2	Without SH storage
3	Without solar thermal plant
4	Without solar thermal plant and DHW storage
5	Without solar thermal plant, DHW/SH storage
6	Without heat pump
7	Without internal combustion engine
Configuration	Other cases
8	Gas turbine instead of internal combustion engine
9	Conventional energy supply system

4.3.1. Single-objective optimization for different configurations of the DES

In order to show the contribution of each energy device in reducing energy costs and CO_2 emission separately, the economic and environmental impact optimizations are carried out for different configurations of the DES. In addition, the daily energy cost and CO_2 emission are also evaluated for one of the most common conventional energy supply systems, consisting of the power grid to meet the electricity demand, and natural gas boilers to meet the domestic hot water and space heating demands. The configurations are listed in Table 2.

Fig. 8a and 8b show the daily energy cost obtained by the economic optimization and the daily CO_2 emission obtained by the environmental impact optimization, respectively. Configuration 1 is the reference case, consisting of all energy devices shown in Fig. 3. In the reference case (discount on the excise fee of natural gas involved), the minimum energy cost and minimum CO_2 emission are obtained by the economic and environmental impact optimizations, respectively. For Configuration 2, there is a negligible increase in the energy cost and no change in CO_2 emission, compared with those of the reference case. This highlights the small impact of the space heating storage on both the objectives.

Configuration 3 excludes the solar thermal plant. A 3% increase in the energy cost and a 5% increase in the CO_2 emission compared with those of the reference case, respectively, confirm the importance of this energy device for both the objectives. Besides the solar thermal plant, Configurations 4 and 5 exclude the domestic hot water storage and both the thermal storage systems respectively, and results are similar to those obtained for Configuration 3.

Configuration 6 excludes the heat pump. The daily energy cost is 11% higher than that in the reference case. The daily CO_2 emission is 21% higher than those in the reference case. Therefore, the heat pump affects the environmental impacts more than the energy costs, as also shown in Fig. 7c. In the environmental impact optimization, the space heating demand is fully satisfied by the heat pump, whereas in the economic optimization the share of space heating demand satisfied by the heat pump reaches the minimum value.

Configuration 7 excludes the internal combustion engine. The electricity load is fully satisfied by the power grid, and without exhaust gas the heat recovery boilers are fuelled by natural gas. The opposite trends of energy costs and CO_2 emission as compared with those of Configuration 6 are exhibited. The daily energy cost is 25% higher than that in the reference case. However, the daily CO_2 emission is only 0.5% higher than those in the reference case. This is also remarkable in Fig. 7a, since in the environmental impact optimization only 5% of the electricity load is satisfied by the CCHP system.

In Configuration 8, the internal combustion engine is substituted by a gas turbine of the same size. The energy cost is increased

Please cite this article in press as: Marialaura Di Somma, et al., Multi-objective operation optimization of a Distributed Energy System for a large-scale utility customer, Applied Thermal Engineering (2016), doi: 10.1016/j.applthermaleng.2016.02.027

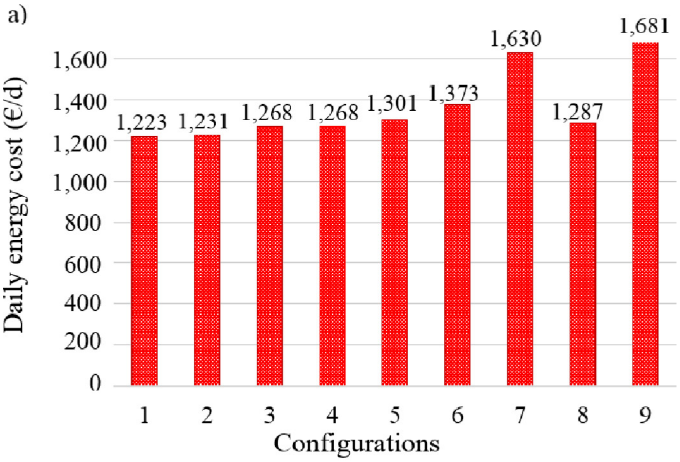

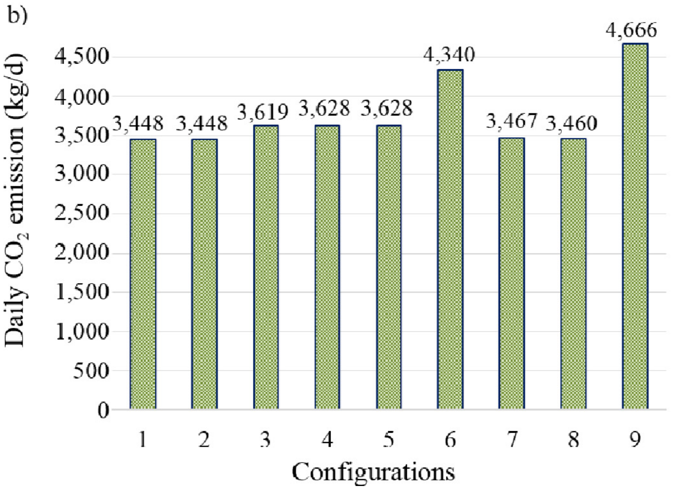

Fig. 8. a) Daily energy cost for Configurations 1–9 in the economic optimization; b) Daily CO_2 emission for Configurations 1–9 in the environmental impact optimization.

by 5% and the CO_2 emission is increased by 0.3%, as compared with those in the reference case, respectively. This confirms that the internal combustion engine is a better solution in terms of costs and environmental impacts than the gas turbine, due to the higher total energy conversion efficiency of the CCHP system with the internal combustion engine than that of the CCHP system with the gas turbine. It can be noticed that the effect of the prime mover change has larger effects on energy costs than environmental impacts.

Finally, for the conventional energy supply system, the daily energy cost and the daily CO_2 emission are 27% and 26% higher than those in the reference case. Results show that the energy cost and the environmental impacts are strongly reduced by the optimized operation of the DES.

4.3.2. *Multi-objective optimization for different configurations of the DES*

The multi-objective optimization is carried out for some configurations among those listed in Table 2, to compare the Pareto fronts with that obtained in the reference case (red Pareto front in Fig. 6). The Pareto fronts for Configurations 3, 6, 8, as well as for the reference case are presented in Fig. 9.

For Configuration 3 (without solar thermal plant), the Pareto front is similar to that in the reference case, especially in the left side (ω is close to 1). The CO_2 emission is highly reduced (10%) from $\omega = 1$ to 0.9, with a negligible increase in the energy cost (0.31%). When the weight of the environmental objective increases over that of the economic one (right side), the slope of the Pareto front is lower than that of the reference case. This means that when more attention is paid to the environmental performance, the rate of the energy cost increase is larger than that of CO_2 emission reduction, as compared with the reference case. The daily energy costs obtained by the economic and environmental impact optimizations are 24% and 22% lower than those obtained with the conventional energy supply system (Configuration 9).

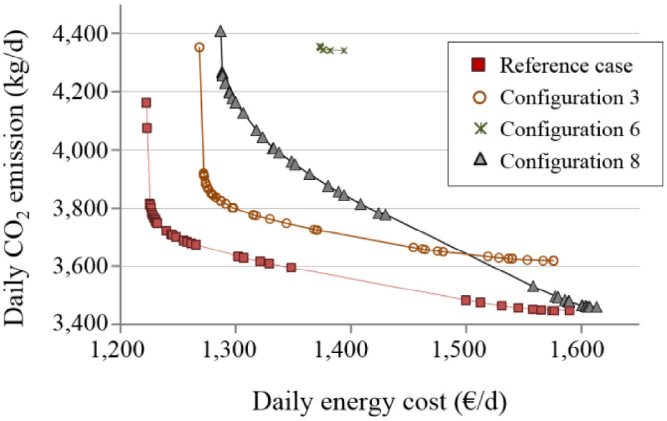

Fig. 9. Pareto fronts for Configurations 3, 6, 8 and Reference case.

For Configuration 6 (without heat pump), very few trade-offs points are obtained. The difference between the maximum and minimum daily energy cost obtained by the environmental impact and economic optimization, respectively, is only 1.5%. The difference between the maximum and minimum daily CO_2 emission obtained by the economic and environmental impact optimizations is only 0.34%. This is because of the flat shape of the Pareto front, which implies a negligible reduction in CO_2 emission with a significant increase in the energy cost. Daily energy costs obtained by the economic and environmental impact optimization are 18% and 7% lower than those obtained with the conventional energy supply system (Configuration 9).

For Configuration 8 (gas turbine generator instead of internal combustion engine), the shape of the Pareto front is different from that in the reference case. The slope of the Pareto front changes more quickly than that of the Pareto front in the reference case. When ω changes from 1 to 0.9, there is a negligible increase in the energy cost (0.12%), and the reduction in the CO_2 emission is about 3.4%. The daily energy costs obtained by the economic and environmental impact optimizations are 23% and 26% lower than those obtained with the conventional energy supply system (Configuration 9).

5. Conclusions

In this paper, a multi-objective linear programming problem is formulated to obtain the optimized operation strategies of a Distributed Energy System (DES) to reduce both the energy cost and environmental impacts, while satisfying given time-varying user demands. The Pareto front, consisting of the best possible trade-offs between the daily energy cost and CO_2 emission, is obtained by minimizing a weighted sum of the economic and environmental objectives by using branch-and-cut. Results show that the operation of the DES is sensitive to the weights assigned to the two objectives. The operators of DESs can choose the operation strategy from the Pareto front based on their cost and environmental priorities. The contributions of each energy device in reducing energy costs and CO_2 emissions are evaluated by a sensitivity analysis. In

Please cite this article in press as: Marialaura Di Somma, et al., Multi-objective operation optimization of a Distributed Energy System for a large-scale utility customer, Applied Thermal Engineering (2016), doi: 10.1016/j.applthermaleng.2016.02.027

addition, the Pareto fronts for different configurations of the DES are also discussed. The optimized operation of the DES in the reference case allows to maximize the reduction in terms of costs (27%), and CO_2 emission (26%) as compared with conventional energy supply systems.

Acknowledgements

The authors thank the Università degli Studi di Napoli Federico II for funding this study within an agreement with the University of Connecticut and the Smart grid con sistemi di poligenerazione distribuita (Poligrid).

Nomenclature

A	Area [m^2]
c	Constant in Eq. (16) [kg_{CO2}/€]
COP	Coefficient of performance
$Cost$	Total energy cost [€]
$\dot{E}$	Electricity rate [kW]
E_{cin}	Carbon intensity of power grid [kg_{CO2}/kWh]
Env	Environmental impact [kg_{CO2}]
F_{obj}	Objective function
$\dot{G}$	Natural gas volumetric flow rate [Nm^3/h]
G_{cin}	Carbon intensity of natural gas [kg_{CO2}/kWh]
$\dot{G}_T$	Total solar irradiance [kW/m^2]
$\dot{H}$	Heating rate [kW]
H	Thermal energy [kWh]
k	Generation level of the energy device [kW]
LHV_{gas}	Lower heat value of gas [kWh/Nm^3]
P_{gas}	Natural gas price [€/Nm^3]
P_{grid}	Electricity price [€/kWh]
$\dot{Q}_{ICE,ex}$	Heat rate made available by the exhaust gas [kW]
t	Time [h]
x	Binary decision variable

Greek symbols

Δt	Length of the time interval [h]
η	Efficiency
μ	Percent heat loss rate of the internal combustion engine
ξ	Internal combustion engine exhaust fraction
ω	Weight in Eq. (16)

Superscript/Subscripts

abs	Absorption chiller
boil	Boiler
buy	Bought
CCHP	Combined cooling, heating and power
coll	Collector
dem	Demand
DHW	Domestic hot water
di	Directly provided by natural gas
e	Electricity
ED	Energy device
ex	Exhaust gas
HP	Heat pump
HR	Heat recovery
ICE	Internal combustion engine
in	Input
max	Maximum
min	Minimum
out	Output
SC	Space cooling
SH	Space heating
solar	Solar
sto	Thermal storage

Acronyms

CCHP	Combined cooling, heating and power
DES	Distributed Energy System
DHW	Domestic hot water
ICE	Internal combustion engine
SC	Space cooling
SH	Space heating

References

[1] K. Alanne, A. Saari, Distributed energy generation a sustainable development, Renew. Sustain. Energy Rev. 10 (6) (2006) 539–558.

[2] M.F. Akorede, H. Hizam, E. Poresmaeil, Distributed energy resources and benefits to the environment, Renew. Sustain. Energy Rev. 14 (2010) 724–734.

[3] G. Pepermans, J. Driesen, D. Haesoldoncklx, R. Belmans, W. D'haeseleer, Distributed generation: definition, benefits and issues, Energy Policy 33 (2005) 787–798.

[4] S.R. Allen, G.P. Hammond, M.C. McManus, Prospects for and barriers to domestic micro-generation: a United Kingdom perspective, Appl. Energy 85 (6) (2008) 528–544.

[5] P. Siano, G. Graditi, M. Atrigna, A. Piccolo, Designing and testing decision support and energy management systems for smart homes, J. Ambient Intell. Humaniz. Comput. 4 (6) (2013) 651–661. ISSN 1868-5137.

[6] M.L. Di Silvestre, G. Graditi, E.R. Sanseverino, A generalized framework for optimal sizing of Distributed Energy Resources in micro-grids using an Indicator-Based Swarm Approach, IEEE Trans. Industr. Inform. 10 (2014) 152–162. ISSN 1551-3203.

[7] R. Aringhieri, F. Malucelli, Optimal operations management and network planning of a district system with a combined heat and power plant, Ann. Oper. Res. 120 (2003) 173–199.

[8] V. Dorer, R. Weber, A. Weber, Performance assessment of fuel cell micro-cogeneration systems for residential buildings, Energy Build. 37 (2005) 1132–1146.

[9] A.D. Hawkes, M.A. Leach, Cost-effective operating strategy for residential micro-combined heat and power, Energy 32 (5) (2007) 711–723.

[10] M. Houwing, A.N. Ajah, P.W. Heijnen, I. Bouwmans, P.M. Herder, Uncertainties in the design and operation of distributed energy resources: the case of micro-CHP systems, Energy 33 (10) (2008) 1518–1536.

[11] T. Wakui, R. Yokoyama, K. Shimizu, Suitable operational strategy for power interchange operation using multiple residential SOFC (solid oxide fuel cells) cogeneration systems, Energy 35 (2) (2010) 740–750.

[12] B. Yan, P.B. Luh, B. Sun, C. Song, C. Dong, Z. Gan, et al., Energy-efficient management of eco-communities, IEEE Int. Conf. Automation Sci. Eng. (CASE) (2013) 106–111.

[13] X. Guan, Z. Xu, Q. Jia, Energy-efficient buildings facilitated by microgrid, IEEE Trans. Smart Grid 1 (2011) 466–473.

[14] A. Alarcon-Rodriguez, G. Ault, S. Galloway, Multi-objective planning of distributed energy resources: a review of the state-of-the-art, Renew. Sustain. Energy Rev. 14 (2010) 1353–1366.

[15] H. Ren, W. Zhou, K. Nakagami, W. Gao, Q. Wu, Multi-objective optimization for the operation of distributed energy systems considering economic and environmental aspects, Appl. Energy 87 (12) (2010) 3642–3651.

[16] X.Q. Kong, R.Z. Wang, X.H. Huang, Energy optimization for a CCHP system with available gas turbines, Appl. Therm. Eng. 25 (2005) 377–391.

[17] Educogen, The European Educational Tool on Cogeneration, second ed., 2001.

[18] EPBD Buildings Platform, Country Reports, 2008. ISBN 2-930471-29-8. Available from: <http://www.epbdca.org/Medias/Pdf/EPBD_BuPLa_Country_reports.pdf>.

[19] Hotel Energy Solutions, Analysis on Energy Use by European Hotels: Online Survey and Desk Research, Hotel Energy Solutions Project Publications, 2011. Available from: <http://hes.unwto.org/sites/all/files/docpdf/analysisonenergyusebyeuropeanhotelsonlinesurveyanddeskresearch2382011-1.pdf>.

[20] RESILIENT Project, FP7 RESILIENT Project Consortium. Grant Number #314671. Available from: <http://www.resilient-project.eu/>.

[21] Dispositivi, tecniche e tecnologie abilitanti per le **F**onti **E**nergetiche **R**innovabili verso la **G**reen **E**conomy. FERGE PON Campania, PON03PE_00177_1, funded by Ministry of Education, University and Research.

[22] Smart grid con sistemi di poligenerazione distribuita. POLIGRID POR Campania FSE 2007/2013.

[23] M. Rivarolo, A. Greco, A.F. Massardo, Thermo-economic optimization of the impact of renewable generators on poly-generation smart-grids including hot thermal storage, Energy Convers. Manag. 65 (2013) 75–83.

[24] M. Aprile, Caratterizzazione del settore alberghiero in Italia. Report ENEA RSE/2009/162, 2009.

[25] M. Beccali, M. La Gennusa, L. Lo Coco, G. Rizzo, An empirical approach for ranking environmental and energy savings measures in the hotel sector, Renew. Energy 34 (2009) 82–90.

[26] L. Mongibello, N. Bianco, M. Caliano, G. Graditi, M. Musto, Optimal operation of micro-CHP systems for a single-family house in Italy, Appl. Mech. Mater. 492 (2014) 467–472.

[27] Delibera Autorità per l'Energia Elettrica e per il Gas 119/11. Available from: <http://www.autorita.energia.it/allegati/docs/11/119-11arg.pdf>.

Please cite this article in press as: Marialaura Di Somma, et al., Multi-objective operation optimization of a Distributed Energy System for a large-scale utility customer, Applied Thermal Engineering (2016), doi: 10.1016/j.applthermaleng.2016.02.027

[28] Autorità per l'Energia Elettrica e per il Gas. Available from: <http://www.autorita.energia.it/it/prezzi.htm>.

[29] ASHRAE International Weather files for Energy Calculations (IWEC weather files), Users Manual and CD-ROM, American Society of Heating, Refrigerating and Air-Conditioning Engineers, Atlanta, GA, USA, 2001.

[30] IPCC, Guidelines for National Greenhouse Gas Inventories – CO_2 Emissions from Fuel Combustion, Highlights, 2013 ed., IEA, 2013.

[31] GSE, Guida alla Cogenerazione ad Alto Rendimento CAR, first ed., GSE, 2012.

[32] Delibera Autorità per l'Energia Elettrica e per il Gas 16/98. Available from: <http://www.autorita.energia.it/allegati/docs/98/016-98.pdf>.

Please cite this article in press as: Marialaura Di Somma, et al., Multi-objective operation optimization of a Distributed Energy System for a large-scale utility customer, Applied Thermal Engineering (2016), doi: 10.1016/j.applthermaleng.2016.02.027